monkeys. In addition, oxidative stress reactants calreticulin and ceruloplasmin were identified as drusen components by proteome analysis (Table 3). Calreticulin is a stress induced molecular chaperone protein of the endoplasmic reticulum. The protein also affects intracellular Ca^{2+} homoeostasis and can modulate oxidative stress by blocking Ca^{2+} disturbance in the RPE cells (32, 33). On the other hand, ceruloplasmin is a ferroxidase, converting the hydroxyl-radical producing ferrous (Fe^{2+}) iron to the safer ferric (Fe^{3+}) form. Increased expression of ceruloplasmin has been reported in the mouse retina after photo-oxidation (34) and also in sera from AMD patients (35). In addition to these oxidative stress reactants, we observed accumulation of secondary oxidative products, such as 8-hydroxy-deoxyguanosine (8-OHdG) and 4-hydroxy-2-nonenal (4-HNE), in drusen and the surrounding neural retina in affected monkeys (data not shown). These observations indicate that oxidative stress participates in the pathogenesis of late onset macular degeneration in monkeys, as has been suggested in AMD.

Immunohistochemical studies of drusen composition also demonstrated that monkey drusen of late onset and early onset macular degeneration monkeys contained common components with drusen in AMD (Fig. 2). Drusen of late onset monkeys are observed in animals ranging in age from 13 to 25 yr, while drusen in early onset monkeys appear around the age of 2 yr (1). Recently, Ambati et al. (36) reported knockout mice lacking monocyte chemoattractant protein-1 or its cognate gene C-C chemokine receptor developed cardinal features of AMD, including accumulation of lipofuscin in RPE, photoreceptor atrophy, and choroidal neovascularization. Complement and IgG deposition in the RPE and choroid accompanies senescence in this model. The authors suggest that impaired macrophage recruitment may allow accumulation of C5a and IgG, leading to abnormal complement activation. A similar genetic defect that promotes the initiation of local chronic inflammation could be the cause of degeneration in the early onset monkeys. Further study of the molecular properties of drusen and identification of the disease-causing gene may provide important clues to the common causal events that trigger abnormal complement activation and subsequent drusen formation in AMD.

Involvement of anti-retinal autoimmunity against annexin II and μ-crystallin for late onset macular degeneration monkeys was also described in this study (Fig. 4). A previous report localized annexin II to the basal plasma membrane of the RPE (23). Moreover, this report identified annexins (annexin I, II, V, and VI) as drusen components in AMD. Annexin V was also identified in this study by proteome analysis of drusen composition as shown in Table 3. A possible pathological pathway whereby autoimmunity against annexin II could contribute to drusen formation is the following: *1*) anti-annexin II immunoglobulins bind to the basal plasma membrane of the RPE; *2*) the inactive C1 serum protein interacts with the Fc portion of the immunoglobulin; *3*) this leads to formation of the C5b9 membrane attack complex; and *4*) causing damage to the RPE cells followed by shedding of the cell membranes in the sub-RPE space. Immune complex formation might continue in the resultant drusen cores leading to further development of drusen.

Alternatively, anti-annexin II autoantibodies might contribute to the pathogenesis of the disease by impairing the normal functions of the protein. Annexins are Ca^{2+} and phospholipid binding proteins containing the annexin repeat motif and have been shown to interact with various ligands both outside and inside the cells to play multiple biological roles including the control of inflammatory responses (37). Annexin I is known to function as an anti-inflammatory mediator because of its response to glucocorticoids (38) and its activities in several animal models of inflammation (39, 40). Furthermore, high levels of anti-annexin autoantibodies have also been

reported in sera from patients with the common chronic inflammatory disease rheumatoid arthritis (RA) (41, 42). Continuous production of annexin autoantibodies that accelerate the inhibition of anti-inflammatory activity is suspected of contributing for the pathogenesis of RA. Similar mechanisms might be involved in the induction and maintenance of chronic inflammation in late onset macular degeneration monkeys.

Translocation of different annexins from the plasma membranes of phagocytic cells to the maturing phagosome membranes is believed to be involved in phagocytosis (37, 43). RPE cells perform numerous tasks essential for visual function, such as recycling of 11-*cis*-retinal for rod opsin, forming a barrier between the neural retina and the choroid, providing nutrients to the photoreceptors, and phagocytosis of rod photoreceptor outer segments. Disturbance of this latter process is likely to cause accumulation of debris and lead to retinal degeneration. Previous reports have shown that phagocytosis by RPE can be inhibited by an antiserum to RPE cell plasma membrane (44). Autoantibodies against annexin II could be one such inhibitory factor and may contribute to the pathogenesis of disease in late onset monkeys.

Several affected monkeys showed considerably elevated antibody titer against μ-crystallin compared with the control group (Fig. 4*F*). Crystallins are proteins expressed in very high abundance in the lens that are critical to the refractivity and transparency of the organ. μ-Crystallin is a taxon specific crystallin first described as a lens protein in several Australian marsupials (45). It binds NADPH is related to enzymes involve in aminoacid metabolism and is also expressed in photoreceptors and RPE. Other crystallins are also known to be synthesized by both the neurosensory retina and RPE, possibly functioning as stress proteins. Recently, crystallins were described as among the common proteins of drusen in human AMD (23). Our observations confirm crystallins are present in monkey drusen (Table 3). It can be hypothesized that injured RPE cells shed their cell membranes with cytoplasmic μ-crystallin into sub-RPE space exposing as new autoantigens. However, in this study, μ-crystallin expression was limited in the neural retina of normal control monkey compared with RPE (data not shown). One explanation of this discrepancy is that RPE cells compromised by some physical or metabolic stress might newly express μ-crystallin; in that case, the appearance of anti-μ-crystallin autoantibodies may be considered as a secondary event after RPE cell injury caused by chronic complement attack.

It still remains unclear whether autoantibodies against annexin II or μ-crystallin are the initial cause of the disease. It is possible that autoimmunity against these proteins might be the most critical event in the retina because annexin II is a ubiquitous protein and μ-crystallin is also expressed in brain, muscle, and kidney (46). Detailed clinical information on immunity in individual monkeys is essential to determine the primary cause of this disease. Although further analyses are required to define the relationship between the autoantibodies and the pathogenesis of the disease, autoantigens identified in this study strongly suggest the involvement of anti-retinal autoimmunity in AMD. Defining the AMD- related autoantibodies may provide possible diagnostic tools for the early detection and management of AMD.

ACKNOWLEDGMENTS

This work was supported by research grant, Research on Measures for Intractable Diseases, Ministry of Health, Labor and Welfare of Japan (Iwata) and by the fellowship of the Promotion of Science for Japanese Junior Scientists (Umeda). We appreciate Dr. Samuel Zigler Jr. of the

National Eye Institute, NIH, for the critical reading of the manuscript.

REFERENCES

1. Umeda, S., Ayyagari, R., Allikmets, R., Suzuki, M. T., Karoukis, A. J., Ambasudhan, R., Zernant, J., Okamoto, H., Ono, F., Terao, K., et al. (2005) Early-onset macular degeneration with drusen in a cynomolgus monkey (Macaca fascicularis) pedigree: exclusion of 13 candidate genes and loci. *Invest. Ophthalmol. Vis. Sci.* **46,** 683–691

2. Vingerling, J. R., Klaver, C. C., Hofman, A., and de Jong, P. T. (1995) Epidemiology of age-related maculopathy. *Epidemiol. Rev.* **17,** 347–360

3. Age-Related Eye Disease Study Research Group. (2001) A randomized, placebo-controlled, clinical trial of high-dose supplementation with vitamins C and E, beta carotene, and zinc for age-related macular degeneration and vision loss: AREDS report no. 8. *Arch. Ophthalmol.* **119,** 1417–1436

4. Stafford, T. J. (1974) Maculopathy in an elderly sub-human primate. *Mod. Probl. Ophthalmol.* **12,** 214–219

5. Ishibashi, T., Sorgente, N., Patterson, R., and Ryan, S. J. (1986) Pathogenesis of drusen in the primate. *Invest. Ophthalmol. Vis. Sci.* **27,** 184–193

6. Stafford, T. J., Anness, S. H., and Fine, B. S. (1984) Spontaneous degenerative maculopathy in the monkey. *Ophthalmology* **91,** 513–521

7. Hope, G. M., Dawson, W. W., Engel, H. M., Ulshafer, R. J., Kessler, M. J., and Sherwood, M. B. (1992) A primate model for age related macular drusen. *Br. J. Ophthalmol.* **76,** 11–16

8. Monaco, W. A., and Wormington, C. M. (1990) The rhesus monkey as an animal model for age-related maculopathy. *Optom. Vis. Sci.* **67,** 532–537

9. Nicolas, M. G., Fujiki, K., Murayama, K., Suzuki, M. T., Mineki, R., Hayakawa, M., Yoshikawa, Y., Cho, F., and Kanai, A. (1996) Studies on the mechanism of early onset macular degeneration in cynomolgus (Macaca fascicularis) monkeys. I. Abnormal concentrations of two proteins in the retina. *Exp. Eye Res.* **62,** 211–219

10. Nicolas, M. G., Fujiki, K., Murayama, K., Suzuki, M. T., Shindo, N., Hotta, Y., Iwata, F., Fujimura, T., Yoshikawa, Y., Cho, F., et al. (1996) Studies on the mechanism of early onset macular degeneration in cynomolgus monkeys. II. Suppression of metallothionein synthesis in the retina in oxidative stress. *Exp. Eye Res.* **62,** 399–408

11. Suzuki, M. T., Narita, H., Cho, F., Fukui, M., and Honjo, S. (1985) (Abnormal findings in the ocular fundi of colony-born cynomolgus monkeys.) *Jikken Dobutsu* **34,** 131–140

12. Suzuki, M. T., Terao, K., and Yoshikawa, Y. (2003) Familial early onset macular degeneration in cynomolgus monkeys (Macaca fascicularis). *Primates* **44,** 291–294

13. Hageman, G. S., Luthert, P. J., Victor Chong, N. H., Johnson, L. V., Anderson, D. H., and

Mullins, R. F. (2001) An integrated hypothesis that considers drusen as biomarkers of immune-mediated processes at the RPE-Bruch's membrane interface in aging and age-related macular degeneration. *Prog. Retin. Eye Res.* **20**, 705–732

14. Mullins, R. F., Russell, S. R., Anderson, D. H., and Hageman, G. S. (2000) Drusen associated with aging and age-related macular degeneration contain proteins common to extracellular deposits associated with atherosclerosis, elastosis, amyloidosis, and dense deposit disease. *FASEB J.* **14**, 835–846

15. Hageman, G. S., Mullins, R. F., Russell, S. R., Johnson, L. V., and Anderson, D. H. (1999) Vitronectin is a constituent of ocular drusen and the vitronectin gene is expressed in human retinal pigmented epithelial cells. *FASEB J.* **13**, 477–484

16. Johnson, L. V., Ozaki, S., Staples, M. K., Erickson, P. A., and Anderson, D. H. (2000) A potential role for immune complex pathogenesis in drusen formation. *Exp. Eye Res.* **70**, 441–449

17. Gurne, D. H., Tso, M. O., Edward, D. P., and Ripps, H. (1991) anti-retinalantibodies in serum of patients with age-related macular degeneration. *Ophthalmology* **98**, 602–607

18. Penfold, P. L., Provis, J. M., Furby, J. H., Gatenby, P. A., and Billson, F. A. (1990) Autoantibodies to retinal astrocytes associated with age-related macular degeneration. *Graefes Arch. Clin. Exp. Ophthalmol.* **228**, 270–274

19. Galbraith, G. M., Emerson, D., Fudenberg, H. H., Gibbs, C. J., and Gajdusek, D. C. (1986) Antibodies to neurofilament protein in retinitis pigmentosa. *J. Clin. Invest.* **78**, 865–869

20. Thirkill, C. E. (2000) Retinal pigment epithelial hypersensitivity, an association with vision loss: RPE hypersensitivity complicating paraneoplastic retinopathies. *Ocul. Immunol. Inflamm.* **8**, 25–37

21. Dumonde, D. C., Kasp-Grochowska, E., Graham, E., Sanders, M. D., Faure, J. P., de Kozak, Y., and van Tuyen, V. (1982) Anti-retinal autoimmunity and circulating immune complexes in patients with retinal vasculitis. *Lancet* **2**, 787–792

22. Mullins, R. F., Aptsiauri, N., and Hageman, G. S. (2001) Structure and composition of drusen associated with glomerulonephritis: implications for the role of complement activation in drusen biogenesis. *Eye* **15**, 390–395

23. Crabb, J. W., Miyagi, M., Gu, X., Shadrach, K., West, K. A., Sakaguchi, H., Kamei, M., Hasan, A., Yan, L., Rayborn, M. E., et al. (2002) Drusen proteome analysis: an approach to the etiology of age-related macular degeneration. *Proc. Natl. Acad. Sci. USA* **99**, 14682–14687

24. Dithmar, S., Sharara, N. A., Curcio, C. A., Le, N. A., Zhang, Y., Brown, S., and Grossniklaus, H. E. (2001) Murine high-fat diet and laser photochemical model of basal deposits in Bruch membrane. *Arch. Ophthalmol.* **119**, 1643–1649

25. Cousins, S. W., Espinosa-Heidmann, D. G., Alexandridou, A., Sall, J., Dubovy, S., and

Csaky, K. (2002) The role of aging, high fat diet and blue light exposure in an experimental mouse model for basal laminar deposit formation. *Exp. Eye Res.* **75**, 543–553

26. Majji, A. B., Cao, J., Chang, K. Y., Hayashi, A., Aggarwal, S., Grebe, R. R., and De Juan, E., Jr. (2000) Age-related retinal pigment epithelium and Bruch's membrane degeneration in senescence-accelerated mouse. *Invest. Ophthalmol. Vis. Sci.* **41**, 3936–3942

27. Weng, J., Mata, N. L., Azarian, S. M., Tzekov, R. T., Birch, D. G., and Travis, G. H. (1999) Insights into the function of Rim protein in photoreceptors and etiology of Stargardt's disease from the phenotype in abcr knockout mice. *Cell* **98**, 13–23

28. Dithmar, S., Curcio, C. A., Le, N. A., Brown, S., and Grossniklaus, H. E. (2000) Ultrastructural changes in Bruch's membrane of apolipoprotein E-deficient mice. *Invest. Ophthalmol. Vis. Sci.* **41**, 2035–2042

29. Rakoczy, P. E., Zhang, D., Robertson, T., Barnett, N. L., Papadimitriou, J., Constable, I. J., and Lai, C. M. (2002) Progressive age-related changes similar to age-related macular degeneration in a transgenic mouse model. *Am. J. Pathol.* **161**, 1515–1524

30. Bressler, N. M., Bressler, S. B., West, S. K., Fine, S. L., and Taylor, H. R. (1989) The grading and prevalence of macular degeneration in Chesapeake Bay watermen. *Arch. Ophthalmol.* **107**, 847–852

31. Bird, A. C., Bressler, N. M., Bressler, S. B., Chisholm, I. H., Coscas, G., Davis, M. D., de Jong, P. T., Klaver, C. C., Klein, B. E., and Klein, R. (1995) An international classification and grading system for age-related maculopathy and age-related macular degeneration. The International ARM Epidemiological Study Group. *Surv. Ophthalmol.* **39**, 367–374

32. Liu, H., Miller, E., van de Water, B., and Stevens, J. L. (1998) Endoplasmic reticulum stress proteins block oxidant-induced Ca2+ increases and cell death. *J. Biol. Chem.* **273**, 12858–12862

33. Liu, H., Bowes, R. C., III, van de Water, B., Sillence, C., Nagelkerke, J. F., and Stevens, J. L. (1997) Endoplasmic reticulum chaperones GRP78 and calreticulin prevent oxidative stress, Ca2+ disturbances, and cell death in renal epithelial cells. *J. Biol. Chem.* **272**, 21751–21759

34. Chen, L., Dentchev, T., Wong, R., Hahn, P., Wen, R., Bennett, J., and Dunaief, J. L. (2003) Increased expression of ceruloplasmin in the retina following photic injury. *Mol. Vis.* **9**, 151–158

35. Newsome, D. A., Swartz, M., Leone, N. C., Hewitt, A. T., Wolford, F., and Miller, E. D. (1986) Macular degeneration and elevated serum ceruloplasmin. *Invest. Ophthalmol. Vis. Sci.* **27**, 1675–1680

36. Ambati, J., Anand, A., Fernandez, S., Sakurai, E., Lynn, B. C., Kuziel, W. A., Rollins, B. J., and Ambati, B. K. (2003) An animal model of age-related macular degeneration in senescent Ccl-2- or Ccr-2-deficient mice. *Nat. Med.* **9**, 1390–1397

37. Gerke, V., and Moss, S. E. (2002) Annexins: from structure to function. *Physiol. Rev.* **82,** 331–371

38. Comera, C., and Russo-Marie, F. (1995) Glucocorticoid-induced annexin 1 secretion by monocytes and peritoneal leukocytes. *Br. J. Pharmacol.* **115,** 1043–1047

39. Cirino, G., Peers, S. H., Flower, R. J., Browning, J. L., and Pepinsky, R. B. (1989) Human recombinant lipocortin 1 has acute local anti-inflammatory properties in the rat paw edema test. *Proc. Natl. Acad. Sci. USA* **86,** 3428–3432

40. Yang, Y., Leech, M., Hutchinson, P., Holdsworth, S. R., and Morand, E. F. (1997) Antiinflammatory effect of lipocortin 1 in experimental arthritis. *Inflammation* **21,** 583–596

41. Dubois, T., Bisagni-Faure, A., Coste, J., Mavoungou, E., Menkes, C. J., Russo-Marie, F., and Rothhut, B. (1995) High levels of antibodies to annexins V and VI in patients with rheumatoid arthritis. *J. Rheumatol.* **22,** 1230–1234

42. Rodriguez-Garcia, M. I., Fernandez, J. A., Rodriguez, A., Fernandez, M. P., Gutierrez, C., and Torre-Alonso, J. C. (1996) Annexin V autoantibodies in rheumatoid arthritis. *Ann. Rheum. Dis.* **55,** 895–900

43. Kaufman, M., Leto, T., and Levy, R. (1996) Translocation of annexin I to plasma membranes and phagosomes in human neutrophils upon stimulation with opsonized zymosan: possible role in phagosome function. *Biochem. J.* **316,** 35–42

44. Gregory, C. Y., and Hall, M. O. (1992) The phagocytosis of ROS by RPE cells is inhibited by an antiserum to rat RPE cell plasma membranes. *Exp. Eye Res.* **54,** 843–851

45. Wistow, G., and Kim, H. (1991) Lens protein expression in mammals: taxon-specificity and the recruitment of crystallins. *J. Mol. Evol.* **32,** 262–269

46. Kim, R. Y., Gasser, R., and Wistow, G. J. (1992) mu-crystallin is a mammalian homologue of Agrobacterium ornithine cyclodeaminase and is expressed in human retina. *Proc. Natl. Acad. Sci. USA* **89,** 9292–9296

Received February 27, 2005; accepted June 21, 2005.

Table 1

Antibodies used in immunohistochemical studies and conditions of antigen retrieval treatments

Antigen	Retrieval Treatment	Primary Antibody		
		Host	Dilution	Supplier
Amyloid P Component	Pro K	Rabbit	200	Dako, Carpenteria, CA
Apolipoprotein E	-	Mouse	200	Biogenesis, Poole, UK
C5	Pro K	Rabbit	200	Dako, Carpenteria, CA
C5b-9	Pro K	Mouse	50	Dako, Carpenteria, CA
MCP	Autoclave	Rabbit	50	Santa Cruz, Santa Cruz, CA
Vitronectin	-	Mouse	100	Chemicon, Temecula, CA

Table 2

Macular status of aged monkeys

Grade	Examined Year			Total	Percentage
	2001	2003	2004		
Normal	**45**	**98**	**45**	**188**	**67.6%**
Mild	4	11	15	30	10.8%
Moderate	5	16	10	31	11.2%
Severe	6	17	6	29	10.4%
Total	60	142	76	278	100.0%

Two-hundred and seventy-eight aged female monkeys were examined by fundus scope and classified into 4 grades. Normal: macula with no detectable pigmentary abnormalities. Mild: fewer than 5 yellowish-white spots. Moderate: 5 to 20 spots. Severe: more than 20 spots.

Table 3

Protein components in monkey drusen

Protein	Accession No.	Protein	Accession No.
Actin, α 2	gi|4501883|	**Hemoglobin, β**	gi|4504349|
Albumin	gi|4502027|	*Hemoglobin, delta*	gi|70353|
Aldehyde dehydrogenase 3	gi|283971|	*Histone, H2A C*	gi|4504239|
Aldehyde dehydrogenase 5	gi|105247|	*Histone, H2A Z*	gi|4504255|
Aldolase A	gi|4557305|	*Histone, H2B F*	gi|10800140|
Alpha-1-antitrypsin	gi|1703025|	*Ig, α 2C*	gi|113585|
Alpha-1B-Glycoprotein	gi|46577680|	**Ig, gamma 2C**	gi|121043|
Annexin V	gi|4502107|	**Ig, lambda**	gi|87890|
Apolipoprotein E	gi|4557325|	Lactate dehydrogenase A	gi|5031857|
ATP synthase α chain, mitochondrial	gi|4757810|	Malate dehydrogenase 1	gi|5174539|
Calmodulin 2	gi|4502549|	Peptidylprolyl isomerase A isoform 1	gi|10863927|
Calreticulin	gi|4757900|	Phosphoglycerate kinase 1	gi|4505763|
cAMP-dependent protein kinase inhibitor, β	gi|14210480|	Phosphoinositide 3-kinase, T96	gi|7434348|
Cell adhesion protein SQM1	gi|105595|	Plectin 1	gi|14195007|
Ceruloplasmin	gi|4557485|	Prostatic binding protein	gi|4505621|
Clusterin	gi|4502905|	Protease inhibitor 4	gi|21361302|
Collagen, α 1(VII)	gi|627406|	Pyruvate dehydrogenase	gi|4885543|
Complement component 5	gi|4502507|	Pyruvate kinase, M1 isozyme	gi|20178296|
Complement component 9	gi|4502511|	Ran binding Protein 2	gi|1709217|
Creatine kinase B	gi|125294|	Recoverin	gi|4506459
Crystallin, β B2	gi|299263|	Retinol binding protein 3	gi|4506453|
Crystallin, β S	gi|345764|	Structural maintenance of chromosomes 1-like 1	gi|30581135|
Dystrobrevin, α isoform 8	gi|14916515|	Transferrin	gi|4557871|
Enolase 2	gi|5803011|	Triosephosphate isomerase 1	gi|4507645|
G3PDH	gi|7669492	*Tubulin, α 3*	gi|5174733|
Glucose phosphate isomerase	gi|18201905|	Ubiquitin and ribosomal protein L40	gi|4507761|
Glutamate-ammonia ligase	gi|2144562|	Ubiquitous mitochondrial creatine kinase	gi|10334859|
Haptoglobin	gi|4826762|	**Vimentin**	gi|14742600|
Haptoglobin-related protein	gi|123510|	**Vitronectin**	gi|72146|
Hemoglobin, α 2	gi|4504345|	14-3-3 protein β/α	gi|4507949|

The components consistent with those of AMD drusen are shown in bold letters. The components that belong to the gene families, other members of which are known to be constituents of drusen in AMD, are shown in italic letters. National Center for Biotechnology Information database accession and version numbers are listed.

Fig. 1

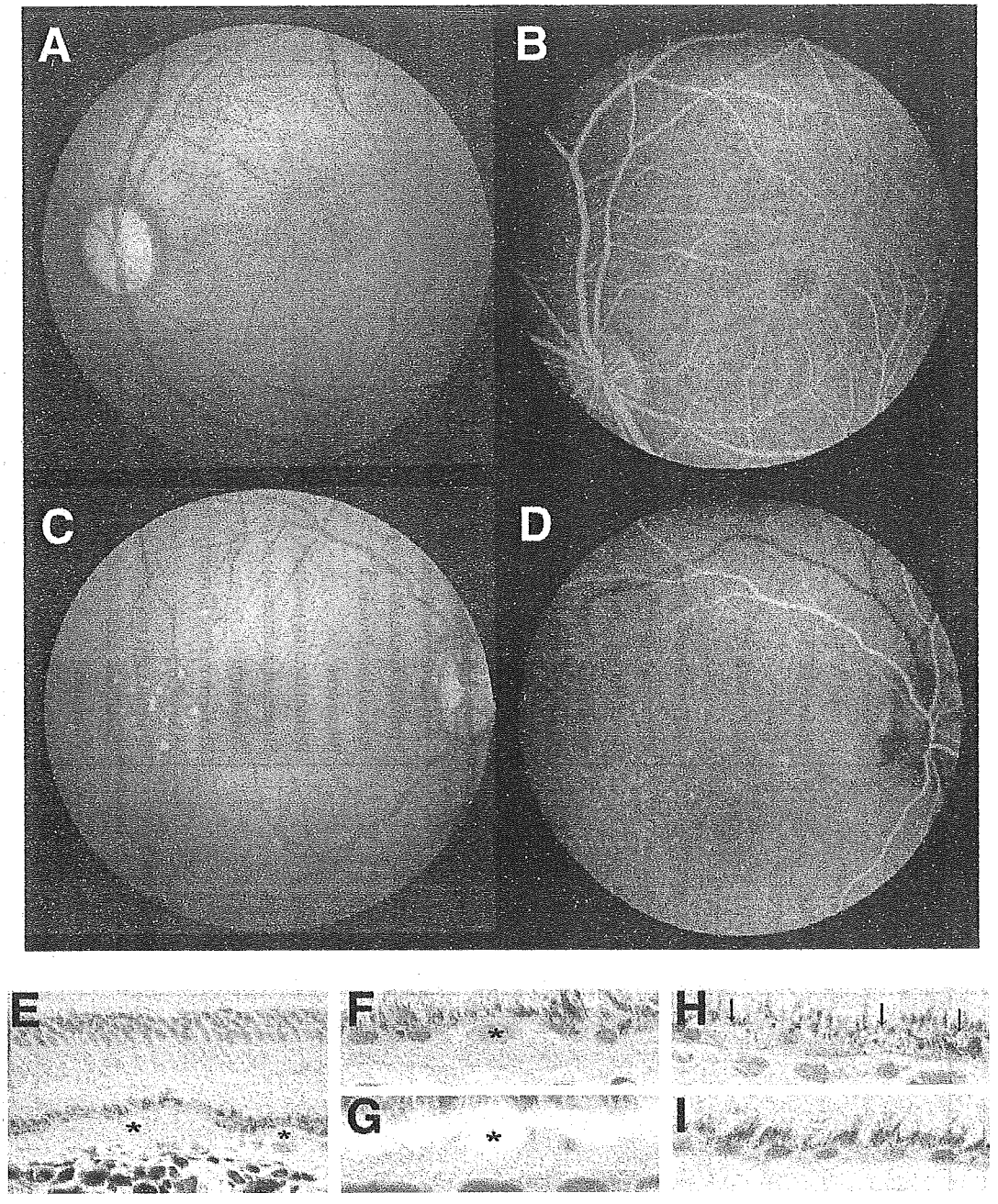

Figure 1. Drusen and degenerative changes of the RPE cells in late onset macular degeneration monkeys. Fundus photographs (*A*, *C*) and fluorescein angiography (FA) (*B*, *D*) of monkeys affected with late onset macular degeneration. Fine dots colored in yellowish-white could be observed in maculae (*A*, *C*). Hyperfluorescein dots could be detected by FA corresponding to these spots (*B*, *D*). Fundus photograph and FA of a 17-year-old monkey that showed vacuolation and hyper- or hypopigmentation of the RPE cells (*A*, *B*). The fundus photograph and FA of another 17-year-old monkey that showed drusen (*C*, *D*). No abnormalities were found in the optic disc nor the blood vessels. *E*) Various sized drusen accumulated between the RPE and choriocapillaris in the macular region (asterisks). Photoreceptor inner and outer segments appeared largely normal. *F*) Drusen that had an eosinophilic inclusion (asterisk). *G*) This spherical structure showed equivalent autofluorescence to that emitted by lipofuscin granules in the RPE (asterisk). *H*) Vacuolation and hyper- or hypopigmentation of the RPE cells (arrows). *I*) Intact region of the RPE in the same monkey as *H*.

Fig. 2

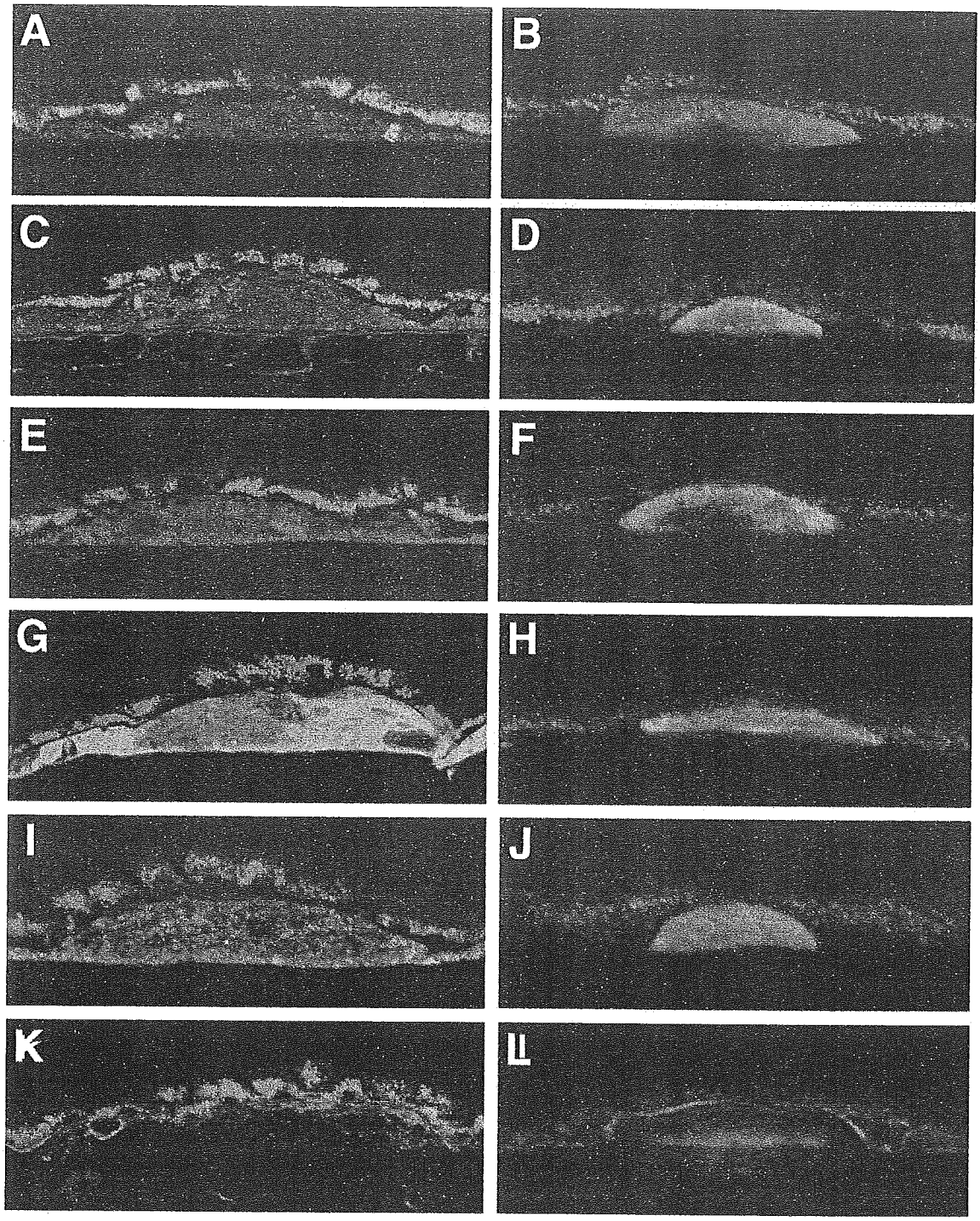

Figure 2. Drusen both in late onset and early onset macular degeneration monkeys are immun-reactive for protein components known in human AMD. Drusen in late onset (*A*, *C*, *E*, *G*, *I*, *K*) and early onset (*B*, *D*, *F*, *H*, *J*, *L*) macular degeneration were heterogeneously bound by antibodies directed against apolipoprotein E (*A*, *B*), amyloid P component (*C*, *D*), complement component C5 (*E*, *F*), the terminal C5b-9 complement complex (*G*, *H*), vitronectin (*I*, *J*), and membrane cofactor protein (*K*, *L*). Double-labeled images were generated by the green channel for each antigen and red channel for autofluorescence emitted by lipofuscin pigment in the RPE.

Fig. 3

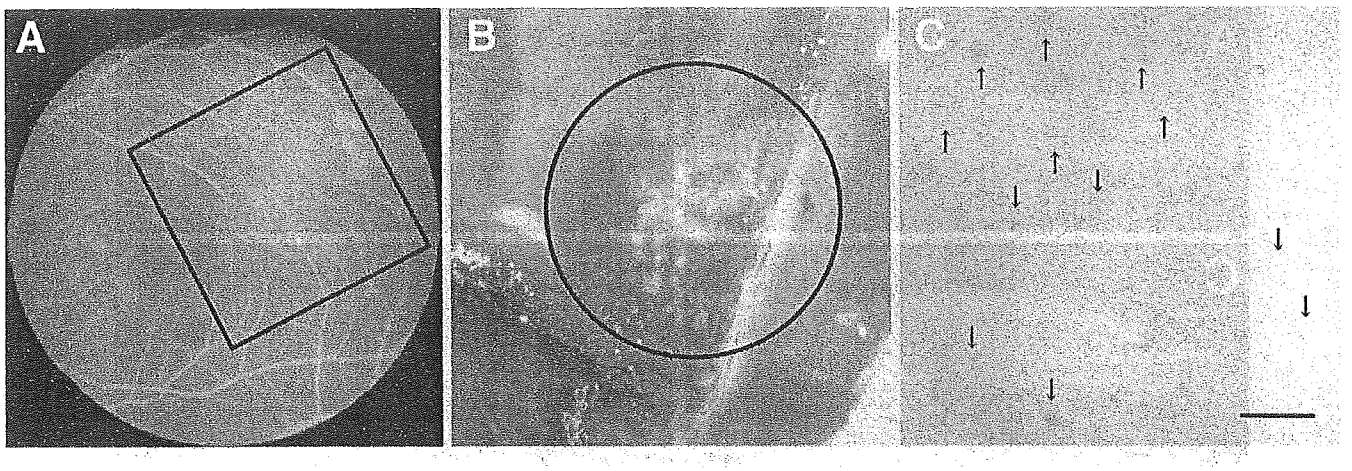

Figure 3. Isolation of drusen. *A*) FA photograph of a monkey retina used for drusen isolation. A number of drusen that show hyperfluorescence could be observed in parafoveal region (indicated by a rectangle). *B*) Drusen could be observed attached to surface of Bruch's membrane at magnifications between 20 and 30 diameters under a stereoscopic microscope (white materials in a circle). *C*) Isolated drusen (arrows). Diameter of a circle in *B* = 3 mm. Bar in *C* = 1 mm.

Fig. 4

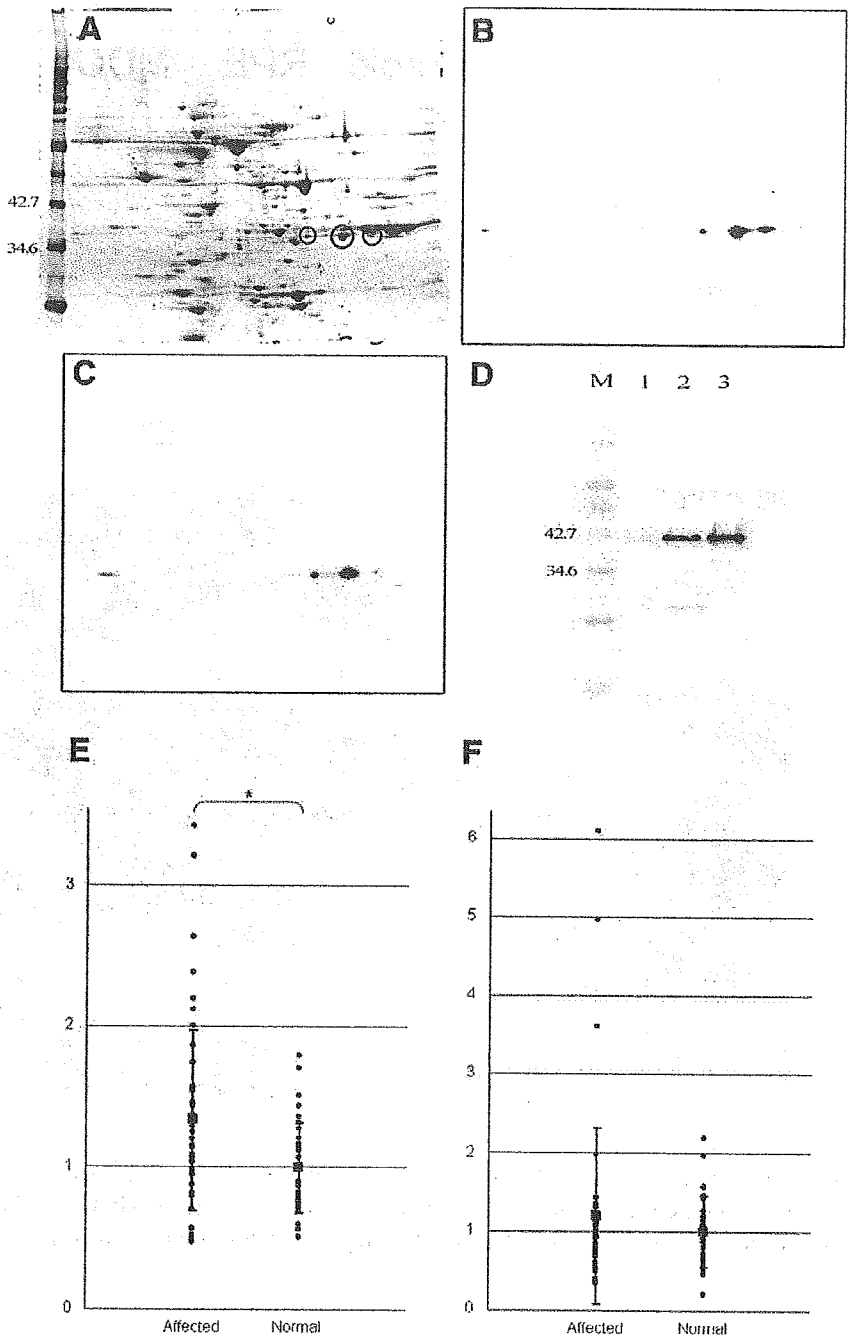

Figure 4. Identification of immunogenic molecules for autoantibodies in the affected monkey sera with late onset macular degeneration. ***A***) 2-D electrophoretic image of retinal proteins visualized by SYPRO Ruby. ***B***) Serum from same monkey in **Fig. 1*C*** showed 3 immunoreactive spots in a row at ~38 kDa. Corresponding protein spots to chemiluminescent signals were excised (circles in ***A***) and analyzed by LC-MS/MS. ***C***) Chemiluminescent signals obtained by immunoreaction with anti-annexin II monoclonal antibodies completely matched those with the serum. ***D***) The affinity purified recombinant annexin ran on SDS-PAGE gel at ~41 kDa (lane 1). Recombinant proteins reacted with both anti-annexin II monoclonal antibodies (lane 2) and autoantibodies in serum (lane 3). M, molecular size marker (kDa). Relative antibody titers against annexin II (***E***) or μ-crystallin (***F***) in sera from affected monkeys with late onset macular degeneration and age-matched control animals. Relative antibody titers of individual monkeys are indicated by ratio to mean of normal monkeys. **P* value <0.01.

Fig. 5

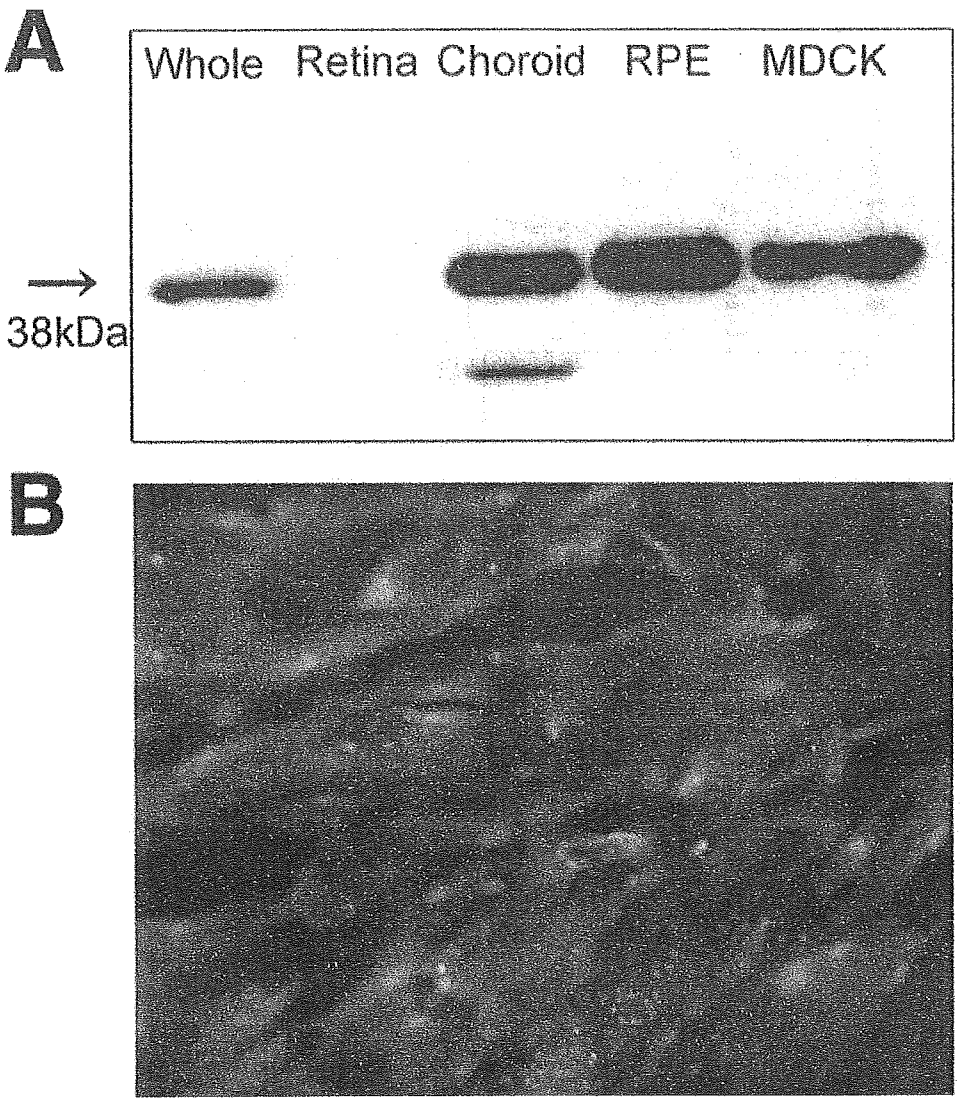

Figure 5. Expression of annexin II in the retina. ***A)*** Protein expression of annexin II (38 kDa) was confirmed in whole retina, choroid, and most intensively in cultured human RPE cells. Protein extract from MDCK cells was used for positive control. ***B)*** Fluorescence microscopy demonstrated that RPE cells highly expressed annexin II in vitro.

J Hum Genet (2005) 50:382–394
DOI 10.1007/s10038-005-0261-9

ORIGINAL ARTICLE

Keiko Tadokoro · Mayu Yamazaki-Inoue
Maki Tachibana · Mina Fujishiro · Kazuaki Nagao
Masashi Toyoda · Miwako Ozaki · Masami Ono
Nobuhiro Miki · Toshiyuki Miyashita · Masao Yamada

Frequent occurrence of protein isoforms with or without a single amino acid residue by subtle alternative splicing: the case of Gln in *DRPLA* affects subcellular localization of the products

Received: 12 May 2005 / Accepted: 17 May 2005 / Published online: 10 August 2005

Abstract Protein isoforms with or without a single amino acid residue make a subtle difference. It has been documented on a few genes that alternative splicing generated such isoforms; however, the fact has attracted little attention. We became aware of a subtle sequence difference in *DRPLA*, a polyglutamine disease gene for dentatorubral pallidoluysian atrophy. Some reported cDNA sequences lacked 3 nucleotides (nt) (CAG), which were positioned apart from the expandable and polymorphic CAG repeats and also coded for glutamine. We experimentally confirmed that the difference was indeed generated by alternative splicing utilizing two acceptors separated by 3 nt. In *DRPLA*, the expression ratio of two mRNA isoforms was almost constant among tissues, with the CAG-included form being major. The glutamine-included protein isoform was more predominantly localized in the nucleus. Database searching revealed that alternative splice acceptors, as well as donors, are frequently situated very close to each other. We experimentally confirmed two mRNA isoforms of 3 nt difference in more than 200 cases by RT-PCR and found interesting features associated with this phenomena. Inclusion of 3 nt tends to result in single amino acid inclusion despite the phase of translational frame. The expression ratio sometimes varied extensively among tissues.

Keywords Subtle alternative splicing · Splice acceptors · Polyglutamine diseases · DRPLA · Subcellular localization

K. Tadokoro · M. Yamazaki-Inoue · M. Tachibana
M. Fujishiro · K. Nagao · M. Toyoda · T. Miyashita
M. Yamada (✉)
National Research Institute for Child Health and Development,
2-10-1 Ohkura, Setagaya-ku, Tokyo 157-8535, Japan
E-mail: myamada@nch.go.jp
Tel.: +81-3-34160181
Fax: +81-3-54947035

M. Tachibana
Department of Pediatrics, Tokyo Medical University,
Tokyo, Japan

M. Fujishiro
Laboratory of Nucleic Acid Science, Nihon University,
Fujisawa, Japan

M. Ozaki
Laboratory for Memory and Learning, Brain Science Institute,
Riken, Wako, Japan

M. Ono · N. Miki
Institute of Clinical Endocrinology, Tokyo Women's
Medical University, Tokyo, Japan

Introduction

Alternative splicing of pre-mRNA is an important regulatory mechanism for quantitative control of gene expression and also for generating diverse protein species (Lopez 1998; Modrek and Lee 2002; Black 2003). It is highlighted, as the human-genome-sequencing project has revealed a limited number of genes (20,000–25,000) in the genome, which were far less than expected for functional complexity (International Human Genome Sequencing Consortium 2004). Recent surveys in databases revealed that as many as 40–60% of human genes are associated with alternative splicing (Black 2003). Three fundamental types of alternative splicing are noted: one is a choice in use of the entire potential exonic sequence (cassette exon or skipped exon) and the other two are selection of the site for a donor or acceptor in the potential continuous exonic sequence. Other types, mutually exclusive exon and intron retention, may be explained by the combination of the fundamental types. The choice for the first exon in alternative splicing is sometimes associated with differential regulation in expression, as regulatory elements are usually situated near the transcriptional start site. Alternative splicing

occurring in the coding region gives rise to generation of protein isoforms. Recent surveys also revealed that 70–88% of alternative splices cause a change in protein products (Black 2003). As one event of alternative splicing in a coding region usually generates a pair of protein isoforms, a multiple combination of alternative splicing events in a gene may generate an enormous number of protein isoforms, sometimes reaching to dozens or even hundreds.

Among diversified protein isoforms, a pair of isoforms with or without a single amino acid residue is the case with a minimum difference. Although it has been documented that such isoforms are generated by alternative splicing on a handful of genes (Manrow and Berger 1993; Condorelli et al. 1994; Vogan et al. 1996; Oberkofler et al. 1997; Lin et al. 2000) (Table 1), the phenomenon seems not to be justly recognized. The difference in amino acid as well as nucleotide sequences is so subtle that it may be disregarded or explained by experimental and/or human errors. We became aware of such a subtle difference in a previously reported cDNA sequence after comparison with sequences that other laboratories reported.

Dentatorubral pallidoluysian atrophy (DRPLA) is an autosomal dominant neurodegenerative disorder characterized by selective neuron loss in the cerebellar and pallidal outflow pathways (Kanazawa 1998). Patients show a combination of ataxia and extrapyramidal signs (chorea and athetosis) to varying degrees. We detected expansion of CAG repeats on chromosome 12p13 in the patients (Nagafuchi et al. 1994a) and then determined the entire cDNA sequence of the gene (Nagafuchi et al. 1994b). Several other neurodegenerative disorders, including Huntington's disease have been shown to be caused by expansion of CAG repeats in the coding region of respective genes (Cummings and Zoghbi 2000). As the CAG unit is situated in the translational frame and encodes glutamine, these disorders are collectively called polyglutamine diseases. It has often been observed through these diseases that the age of onset becomes younger with more severity in successive generations. This phenomenon, genetic anticipation, is now explained by the following two facts. The severity is correlated to the number of repeat iterations, and the extended repeats are further expanded when transmitted to the next generation. DRPLA is typical in genetic anticipation when the extended allele is transmitted paternally (Nagafuchi et al. 1994a; Cummings and Zoghbi 2000). As repeat expansion is a novel type of mutation associated with a subset of disorders and shows unique features, it attracts broad attention. The molecular mechanism underlying cell death has been demonstrated as induction of apoptosis at the final step, and several processes have been proposed for the route where the cohesive force of the polyglutamine tract is central (Okamura-Oho et al. 2003; Michalik and Van Broeckhoven 2003; Forman et al. 2004). In contrast, it is still uncertain how and why specific subsets of neurons are degenerated in respective polyglutamine diseases. To address this issue, we have been studying the normal functions of the *DRPLA* gene and its product.

In this report, we demonstrate an alternative splice in the *DRPLA* gene, which originated from a subtle sequence difference. We characterized the DRPLA protein isoforms with or without a single glutamine residue and found that such a subtle difference affected the protein nature. We extensively searched for similar phenomena in the literature and databases, experimentally examined cases, and revealed widespread occurrence of protein isoforms with or without a single amino acid residue in the human proteome due to alternative splicing. We propose the term of "subtle alternative splicing" for alternative splicing to generate a subtler difference, such as 3 nt, in mRNA and a single amino acid residue in protein.

Materials and methods

RT-PCR

RNA preparations from human, mouse, and rat tissues were purchased form several companies, including BD Biosciences Clontec, and Ambion and RNA from cultured cells and rodent tissue was prepared with a standard method, as described previously (Tadokoro et al. 1993; Miyashita et al. 1997). Fine, dissected, rat brain was performed with the aid of markers and ascertained by other means (Ozaki et al. 2004). One or two microgram of total RNA was subjected to direct cDNA synthesis using Superscript II RNaseH minus reverse transcriptase with the AP primer (an oligo-dT primer with an attached sequence) under the conditions recommended for the 3′-RACE system (Invitrogen, UK). An aliquot of synthesized cDNA was subjected to PCR amplification in a reaction containing 200 μM of each deoxynucleotide triphosphate, 0.5 μM of each primer, and 1 U of rTaq polymerase (Takara-bio). The PCR was carried out with a thermocycler in a cycling condition with an initial denaturation of 4 min at 94°C followed by 25–35 cycles of denaturation at 94°C for 1 min, annealing at Tm −10°C for 1 min, and extension at 72°C for 1 min, with a final extension at 72°C for 4 min (Tadokoro et al. 1993). The amounts of synthesized DNA from respective tissues were primarily adjusted to generate an equal level of *GAPDH* products, but the amounts were sometimes readjusted to facilitate the detection of two products with a 3 nt difference. Amplified PCR products were separated by electrophoresis through a 10% polyacrylamide or 3% SeaKem LE agarose gel (FMC BioProducts) and then detected by silver staining (Bio-Rad, Mississauga, ON, Canada) or ethidium bromide staining. Images were captured through a CCD camera, and the integrated optical density of detected bands was measured by the ImagePro-Plus and GelPro image analysis software (Media Cybernetics, Silver Spring, USA). In a mass screening, the ratio of two products with a 3 nt difference was represented in terms

Table 1 Representative genes with subtle alternative splicing utilizing two acceptor sites separated by 3 nucleotides (nt)

Genes[a]	Accession numbers			Exon	References
	cDNA with 3 nt	cDNA without 3 nt	Genome		
DRPLA	D31840	NM_001940 (U23851)	NT_000012 (U47924)	4–5	This study
GHRHR	–	NM_000823(L01406)	NT_000007(AC005155)	1–2	This study
BAIAP2	BC014020	NM_017450 (AB015019)	NT_000017(AC115099)	9–10	This study
PTMA	M14630	NM_002823(BC022433)	NT_000002(AC073476)	2–3	Manrow et al. (1993)
IGF1R	NM_000875 (X04434)	–	NC_0000156 (AY332722)	13–14	Condorelli et al. (1994)
PAX3	NM_181460 (AY251280)	BC008826	NT_000002 (AC010980)	2–3	Vogan et al. (1996)
PAX7	NM_002584 (X96743)	–	NT_000001 (AL021528)	2–3	Vogan et al. (1996)
LEP	NM_000230 (U43653)	D49487	NT_000007 (AC018635)	2–3	Oberkofler et al. (1997)
Dnmt1	AF162282	NM_010066 (X14805)	NT_039472 (CAAA01059910)	4–5	Lin et al. (2000)
CAST	NM_001750 (D16217)	NM_173061 (U58996)	NT_000005 (AC008906)	27–28	This study
MAN2B1	NM_000528 (U60266)	U05572	NT_000017 (AC010422)	7–8	This study
PSEN2	NM_000447 (L43964)	NM_012486 (U34349)	NT_000001 (AL391628)	10–11	This study
LAP1B	AK001780	NM_015602 (AK021613)	NT_000001 (AL353708)	2–3	ENSG00000143337
NOXO1	AB097667	NM_144603 (BC015917)	NT_037887	2–3	ENSG00000162042
CCL20	NM_004591 (D86955)	U64197	NT_005403	1–2	ENSG00000115009
SGNE1	BC005349	NM_003020 (Y00757)	NT_010194 (AJ290438)	3–4	ENSG00000166922
TGFA	NM_003236 (X70340)	BT006833	NT_022184	2–3	ENSG00000163235
	Nucleotide sequences[b]		Amino acid changes	Expression ratio in tissues[c] (longer/shorter)	
	Splice donor site	Splice acceptor site			
DRPLA	TGAGgtgggaa	gagtcttccctttctacag**CAG**GAACTC	Gln/none	8:2–9:1	
GHRHR	GACCgtgagta	atcctgttcactgtttccag**CAG**GTATTG	Gln/none	2:8	
BAIAP2	ACAAgtaaggg	ttacctgtcccttgtcccag**CAG**CCGAGA	ThrAla/Thr	1:9–0:10	
PTMA	TGCTgtgagtg	atggcctgtttttctgtcgag**GAG**AATGAG	Glu/none	0:10–1:9	
IGF1R	AAAAgtaaggc	tttcctcctctttgctgcag**CAG**GATATG	ThrGly/Arg	7:3–8:2	
PAX3	CAAGgtgagcg	gcccgcctgttctcttaaag**CAG**GTGACA	Gln/none	0:10–10:0	
PAX7	CAGAgtgagtg	tcccacctccacctctgaag**CAG**GTGGCG	Gln/none	0:10–9:1	
LEP	CACGgtaagga	tcctcttcctcctgcatag**CAG**TCAGTC	Gln/none	1:9–10:0	
Dnmt1	CTTTgtaagga	cactttctcttgtttttaag**CAG**TTGAAA	SerVal/Phe	4:6–6:4	
CAST	CTCGgtaagca	cagcattatttacttttcag**CAG**AGTGAC	Gln/none	9:1–10:0	
MAN2B1	GCAGgtcagtg	tccgtcgcctcccccagcag**CAG**GCAAAA	Gln/none	0:10–3:7	
PSEN2	ATGGgtgagta	ttctcttcctggacacccag**AAG**AAGACT	GluGlu/Glu	7:3	
LAP1B	CCAGgtaagaa	gttttctcttcctatattag**CAG**TGAGTG	AlaVal/Val	0:10–10:0	
NOXO1	CAAGgtgagtg	gccctggttcccgccctcag**AAG**ACCCTC	Lys/none	0:10–9:1	
CCL20	GAAGgtaagtg	tcacttttttttttttttag**CAG**CAAGCA	AlaAla/Ala	4:6–9:1	
SGNE1	ACAGgtaacag	aaacctttggctgtttgcag**CAG**ATGATG	AlaAsn/Asn	4:6–8:2	
TGFA	AGTGgtgagtg	tgcatctttcctctccccag**CAG**ACCCGC	AlaAsn/Asn	5:5–9:1	

[a]All the genes listed in this table are human, except for mouse *Dnmt1*, as the structure of the corresponding intron–exon boundary in humans differs from that in the mouse. The phenomena for *PAX3* and *PAX7* were originally identified in mice, but the same phenomena were confirmed to occur in humans in this study

[b]Exon and intron for a longer isoform are indicated with upper and lower cases, respectively. Three nucleotides (nt) excluded in the shorter isoform by alternative splicing (optional 3 nt) are indicated in *bold*. The nucleotides encoding the indicated amino acid residues in the longer form are *underlined*

[c]The expression ratio of the longer to shorter isoform among tissues with a considerable expression level is indicated. When the ratio varied among tissues, the range is given. The figures are rounded out to the nearest whole number to bring the total to ten

of 11 scales from 0:10 to 10:0 (longer form/shorter form) after the figures were rounded out to the nearest whole number to bring the total to ten. When the minor form was detectable in images at 2–4% levels, it was indicated with f:10 or 10:f. The approximate estimation was also done by comparison with a standard picture, which was obtained by the mixture of *DRPLA* DNA fragments with a three nt difference in a defined ratio. The primer sequences for human *DRPLA* are described below, and those for other genes are shown in our Web site at http://www.nch.go.jp/genetics/subtlealtsp/.

DRPLA plasmid construction and splicing reaction

The *DRPLA* minigene pSP-DRPLA4-5 was constructed by insertion of a BglII-PstI fragment (1,893 bp from the 60th nt in exon 4 to the 870th nt in exon 5) derived from pMY1224 (Nagafuchi et al. 1994b) into the BamHI/PstI sites of the pSP65 vector (Promega, Madison, WI, USA). For the splicing reaction, pSP-DRPLA4-5 DNA was linearized by HindIII digestion and in vitro transcribed with SP6 RNA polymerase at 35°C for 3 h. Transcribed RNA was isolated with an RNeasy minikit (QIAGEN, Crawley, UK) and subjected to a splicing reaction with the HelaSplice Nuclear Extract (Promega, WA, USA) at 30°C for 16 h. Heat-inactivated nuclear extracts were used in a control to exclude contaminating sources. Treated RNA was converted to DNA with the R54 primer and amplified with the F42 and R51 primers in the RT-PCR condition described above. The sequences of each primer are as follows: R54: 5′-TGCTTCGGTTGTCCTGGTCGAT-3′; F42: 5′-TGAAAGTGAGGAGACCAATGCAC-3′; R51: 5′-GGAGGGAGACTGTGGCCGAG-3′. The PCR condition was adjusted at 58°C for annealing and 1.0 mM for the Mg concentration, and the product size was 70 bp or 73 bp. To construct *DRPLA* expression plasmid, a similar RT-PCR reaction was carried out with another set of primers—F41 and R54—to generate relatively large PCR products (167 bp or 170 bp). The sequence of the F41 primer was 5′-GGAGATCTCAGAGAGTGAAAGTG-3′. The PCR products were purified with QIAEX II silica gels (QIAGEN), digested with BglII and AvrII at their unique sites on the products, and then inserted into the corresponding sites of pMY1240. The BbsI-BstXI fragments (825 bp or 828 bp) covering the exon 4–5 junction in the resultant plasmid were used to replace the corresponding portion of pEGFP-DRPLA-Q14 or pEGFP-DRPLA-Q71, which were EGFP-tagged DRPLA expression plasmid under the CMV promoter (Miyashita et al. 1998). The Q14 was within the normal range while Q71 was in a disease range. It is noted that four Q are encoded by upstream CAGCAACAGCAA, thus the Q14 construct carries uninterrupted ten CAG repeats. The nucleotide sequences of the constructed plasmid were verified by sequencing. To construct the minigenes with a nucleotide substitution, in vitro mutagenesis was carried out on a PCR fragment, as described previously (Miyashita et al. 1997), and resulting fragments were used to substitute the BamHI/AvrII fragment of pSP-DRPLA4-5.

Cell manipulation

Human cervical carcinoma HeLa cells (ATCC CCL 2) were maintained in a Dulbecco's modified Eagle's medium supplemented with 10% fetal bovine serum, 100 U/ml penicillin, and 100 μg/ml streptomycin (Invitrogen) in a humidified atmosphere of 5% CO_2 at

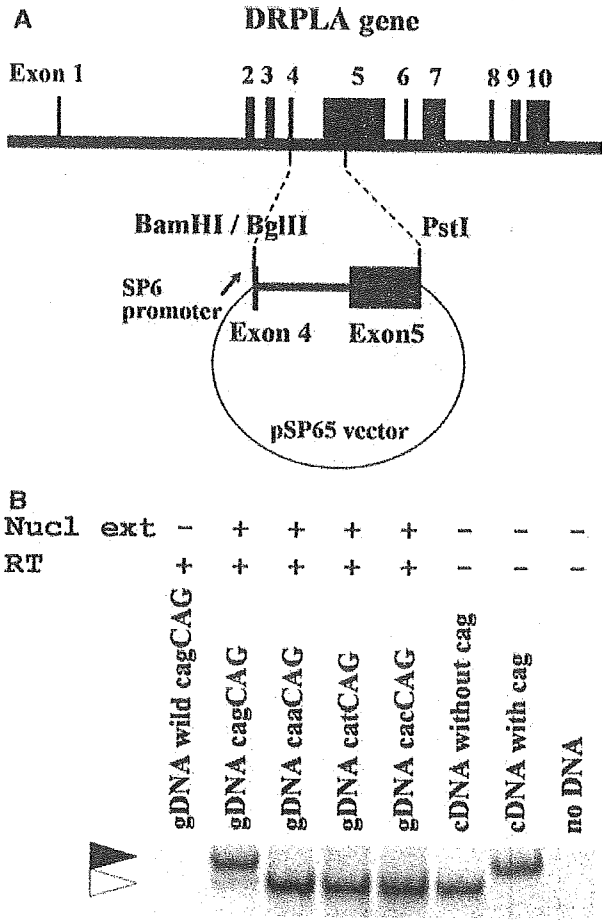

Fig. 1 The subtle difference in the *DRPLA* cDNA sequences caused by alternative splicing. **a** Schematic illustration of a *DRPLA* minigene construct with the genomic organization. pSP-DRPLA4-5 carried genomic DNA, which corresponded to a region from the middle of exon 4 through complete intron 4 to a halfway point in exon 5 under the SP6 promoter. **b** RT-PCR profiles showing generation of two RNA isoforms of 3 nucleotide (nt) difference after splicing reaction. RNA transcribed with the minigene and SP6 RNA polymerase was subjected to the reaction with nuclear extracts followed by RT-PCR. The products were analyzed by electrophoresis in parallel with PCR products generated with each form of cDNA as a reference. The products were confirmed to have expected sequences by sequencing. Heat-inactivated nuclear extracts did not generate spliced forms (*first lane*). After modifying the nucleotide at the −1 position to generate the longer isoform, only the shorter form was produced. *gDNA*, genomic DNA

37°C. Transient transfection was performed with the polycationic liposome method (LipofectAMINE PLUS Reagent, Invitrogen) according to the manufacturer's instructions. To assess the localization of EGFP-DRPLA fusion protein, cells were cultured in poly-d-lysine-coated glass-bottom plates (MatTek) and incubated in a medium containing 50 μM Z-VAD-FMK (Peptide Institute Inc.) after transfection (Miyashita et al. 1997). The cells were observed under a confocal microscope (FLUOVIEW, Olympus), and fluorescent-positive cells were counted in terms of the subcellular localization at the indicated period. The expression levels were ascertained by Western blotting, as described previously (Miyashita et al. 1997).

Database search and analyses

Previous reports on alternative splicing making a subtle difference were searched in Entrez Pub Med at http://www.ncbi.nlm.nih.gov/entrez/query.fcgi. It was generally difficult to find because no common terms have been given for such cases. Nevertheless, we have detected a handful of reports although some others may remain undetected. For a subtle difference in amino acid sequences, we surveyed the ExPASy database (Expert Protein Analysis System) and found a file, humpvar.txt, at http://www.expasy.org/cgi-bin/lists?humpvar.txt, in which information on sequence variants is summarized from the Swiss-Prot human protein sequence entries. Among the list, we selected the cases of "one amino acid missing" and other subtle differences and then ascertained whether it could occur by subtle alternative splicing based on the standard genome and cDNA sequences at the National Center for Biotechnology Information (NCBI). A source data set of humans in the AltSplice database at http://www.ebi.ac.uk/asd/altsplice/ was downloaded and analyzed with database software, Kiri (KanriKogaku Kenkyusho Ltd., Japan). Although we used the prerelease Version 2, the release Version 1 was available after May 21, 2004. Throughout this study, we used genomic sequences to facilitate further analyses although RNA sequences may be more appropriate for splicing.

Results

Subtle alternative splicing in DRPLA

After detection of CAG repeat expansion in DRPLA pedigrees, we determined the entire cDNA sequence of the gene (accession number, D31840, Nagafuchi et al. 1994b). Since then, other laboratories have also reported cDNA sequences for the human *DRPLA* gene and orthologues (U23851, D38529 and others; Onodera et al. 1995; Love et al. 1995; Margolis et al. 1996). It is reasonable to find a difference in the number of iterations of the CAG repeats, which start at the 1,700th position of D31840, as it is polymorphic and expandable. Besides the repeats, the U23851 sequence lacked 3 nt occurring in other sequences (CAG at the 518th position of D31840), which resulted in the absence of the single glutamine residue at 94 in the DRPLA protein (also known as atrophin-1). After the entry of the sequence in the NCBI nucleotide database in 1995, we gradually considered the possibility of alternative splicing, as the inconsistent 3 nt was situated at the boundary of exon 4 and 5. To confirm this, we made a minigene system that contained genomic DNA covering a portion of exon 4, intron 4, and exon 5 under the control of SP6 promoter (Fig. 1). When in vitro transcribed products were subjected to react with nuclear extracts, two products with a 3 nt difference in size were generated. Sequencing verified that the products had the authentic cDNA sequences with or without the CAG nucleotides. This result clearly shows that alternative splicing takes place between exons 4 and 5. As the boundary around the distal end of intron 4 and the proximal start of exon 5 has a structure of cag**CAGGAA**, this result strongly suggests that two positions just after the cag and **CAG** serve as splice acceptors. (Hereafter, nucleotides in intron and exon are indicated with lower and upper cases, respectively, and the target nucleotides that are included or excluded in respective isoforms are indicated by bold upper case.) However, the result may be explained by other type of alternative splicing, for example, inclusion or exclusion of cassette exon consisting of only 3 nt. There are several cag sequences in intron 4, and even one

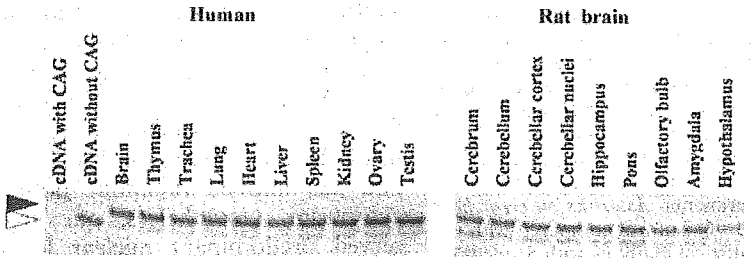

Fig. 2 Expression ratio of two *DRPLA* mRNA isoforms in various tissues. Total RNA from indicated tissues was analyzed by RT-PCR followed by electrophoresis. The PCR products (73 bp and 70 bp) generated with each form of cDNA as a template were loaded in parallel. As *DRPLA* expression levels in tissues varied extensively, the amount of transcribed RNA in RT-PCR was adjusted to give a similar level of PCR products. An almost constant expression ratio of the two transcripts was observed in repeated experiments, with the longer form being major, and representative results are illustrated

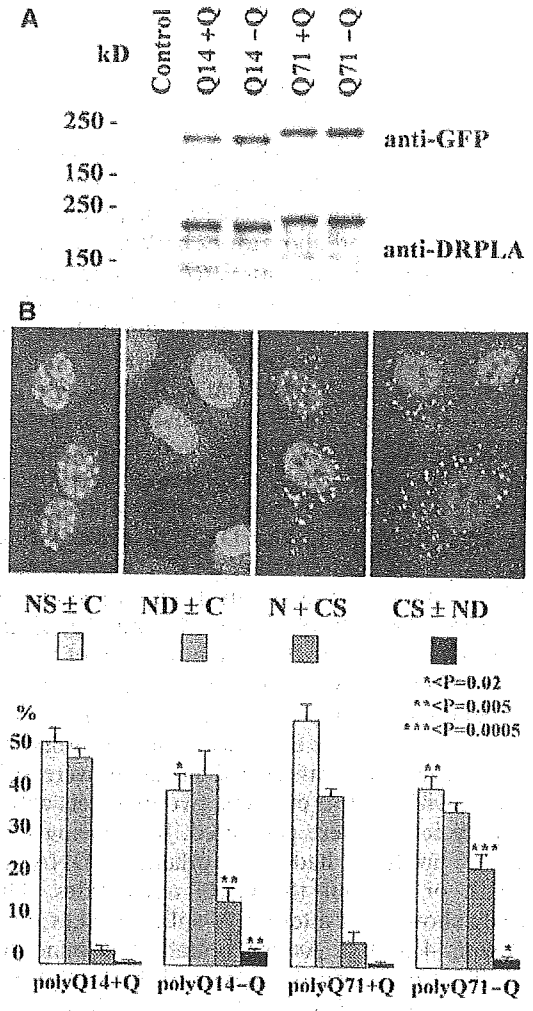

Fig. 3 Subcellular localization of DRPLA protein isoforms with or without a single glutamine residue. HeLa cells were transiently transfected, with one of the constructs carrying *DRPLA* cDNA (full length) tagged with EGFP at its N-terminus. *Q14* and *Q71* indicate the size of the polyglutamine chain (Q14 is within the normal range while Q71 is in a disease range). $+Q$ and $-Q$ indicate inclusion or exclusion of a single glutamine residue at the 94th position by subtle alternative splicing, respectively. **a** Expression levels were ascertained to be almost equal among various constructs by Western blotting with a mouse anti-GFP monoclonal antibody (B-2) or with a rabbit anti-DRPLA polyclonal antibody at 30 h after transfection. **b** Subcellular localization of the EGFP-DRPLA protein isoforms. We classified them into four categories: $NS\pm C$ predominant nuclear localization as a large speckled form (or aggregates) with minor cytoplasmic distribution, $ND\pm C$ predominant nuclear localization as small speckled or diffused forms with minor cytoplasmic distribution, $N+CS$ almost equal distribution in the nucleus and cytoplasm, $CS\pm ND$ predominant cytoplasmic localization with minor nuclear distribution. Typical images are illustrated in the *upper panels*. Respective patterns were counted with 100–200 cells at 30–40 h after transfection and repeated in four independent experiments. *Asterisks on error bars* show a significant difference of the −Q isoform compared with the corresponding +Q isoform by statistical analyses with Student's *t* test

agcag sequence. We substituted the g nucleotide at the −1 position to generate the longer transcript (CAG-included form) with one of the other nucleotides (i.e., caaCAGGAA). The minigene system with such a substitution only generated the shorter transcript. Thus, we conclude that the alternative splicing between DRPLA exons 4 and 5 takes place utilizing two acceptor sites separated by 3 nt.

Expression ratio of two mRNA isoforms of DRPLA

We previously reported with Northern blotting analyses that DRPLA was expressed in a wide variety of tissues (ubiquitous expression), but the extent varied considerably, with the brain, testis, and ovary being relatively high (Nagafuchi et al. 1994b). To distinguish two transcripts including or excluding the CAG sequence, the primer pair was set in exons 4 and 5 to generate relatively short RT-PCR products. The relative amounts of RT-PCR products varied considerably, which was almost consistent to our previous Northern blot results (data not shown). Thus, the amount of reverse-transcribed DNA from each tissue was adjusted so as to generate an almost equal level to easily detect the ratio of the two forms of transcripts. The expression ratio was almost constant among tissues, with the longer form being major (81%–91%) (Fig. 2, *left*). We pursued the possibility that either isoform of transcripts was prominent in the specific area of the brain, and we chose the rat because the size of the brain was large enough to be finely dissected, and the cagCAG structure at the boundary was conserved. The expression ratio of the two isoforms was almost constant among various sections of rat brain, with the longer form being major (79%–88%, Fig. 2, *right*). The result indicates that neither form alone nor the ratio of the two isoforms directly determines the brain area or the subset of neurons in DRPLA pathogenesis. We also analyzed mouse tissue during developmental stages and found consistent results (data not shown).

Characterization of DRPLA protein isoforms

Among the characters of DRPLA protein we were especially interested in the subcellular localization. Many previous reports indicate that DRPLA protein is a shuttle flying across the nuclear membrane (Ross 1997; Miyashita et al. 1998; Igarashi et al. 1998; Okamura-Oho et al. 1999; Miyashita et al. 1999; Ellerby et al. 1999; Yanagisawa et al. 2000; U et al. 2001; Okamura-Oho et al. 2003; Nucifora et al. 2003). DRPLA protein has both the nuclear localization and exclusion signals and has implied functions both in the nucleus and cytoplasm. Nonetheless, our group consistently observed predominant nuclear localization of DRPLA protein with very rare cytoplasmic localization in a variety of culture cells with expression experiments as well as for endogenous protein in staining with antibodies (Miyashita et al. 1998; Okamura-Oho et al. 1999; Miyashita et al. 1999; Yanagisawa et al. 2000; U et al.